Supporting Information

# Development of antibody against drug-resistant respiratory syncytial virus: Rapid detection of mutant virus using split superfolder green fluorescent protein-antibody system

Hyeran Kim[a], Seul Gee Hwang[a], Kyeonghye Guk[a], Yoonji Bae[a], Hwangseo Park[b], Eun-Kyung Lim[a,c*], Taejoon Kang[a*], and Juyeon Jung[a*]

[a]Bionanotechnology Research Center, Korea Research Institute of Bioscience and Biotechnology (KRIBB), Daejeon 34141, Republic of Korea

[b]Department of Nanobiotechnology, KRIBB School of Biotechnology, University of Science and Technology (UST), Daejeon 34113, Republic of Korea

[c]Department of Bioscience and Biotechnology, Sejong University, Seoul 05006, Republic of Korea

*Corresponding author

E-mail: jjung@kribb.re.kr (J. Jung), kangtaejoon@kribb.re.kr (T. Kang), eklim1112@kribb.re.kr (E.-K. Lim)

**Table S1.** Primers for WT RSV F protein production.

| **Primer** | **Sequence (5' → 3')** |
|---|---|
| N-RSVF_*Nhe*I | ATACGCAATTGGCTAGCGATGGAGCTGCTGATCCTGAAG |
| C-RSVF-6H_*Xho*I | AAACATTACCTCGAGTCAGTGGTGGTGGTGGTGGTG |

**Table S2.** Primers for S275F RSV antigen production.

| **Primer** | **Sequence (5' → 3')** |
|---|---|
| N-S275F | CAGAAGAAGCTGATGTTCAACAACGTGCAG ATC |
| C-S275F | GCGCACGATCTGCACGTTGTTGAACATCAGCTTCTT |

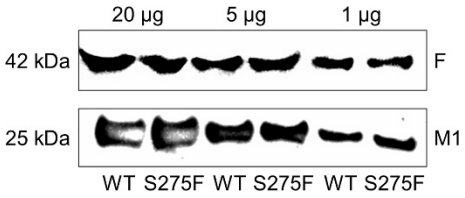


**Figure S1.** Characterization of VLPs containing M1 and RSV F protein by western blots.

**Table S3.** Primers for heavy chain production.

| **Primer** | **Sequence (5' → 3')** |
|---|---|
| LHS39 | GACGAATTCACTCTAACCATGGAA |
| HC LEADER BACK | GGAGTGGACACCTGTAG |
| WH125 | ACTACAGGTGTCCACTCCGAAGTGCAGCTGGTGGAG |
| LHS11 | CACCGGTTCGGGGAAGT |

**Table S4.** Primers for light chain production.

| **Primer** | **Sequence (5' → 3')** |
|---|---|
| LHS42 | TGCAAAGCTTCGGCACGAGCA |
| KC LEADER BACK | TCCTTCAACACCAGACAAC |
| WK125 | TTGTCTGGTGTTGAAGGAGACATCCAGATGACCCAG |
| WK125BSIW1BACK | GCAGCCGCCGTACGTTTGATCTCCACCTTGGTCCCTTG |

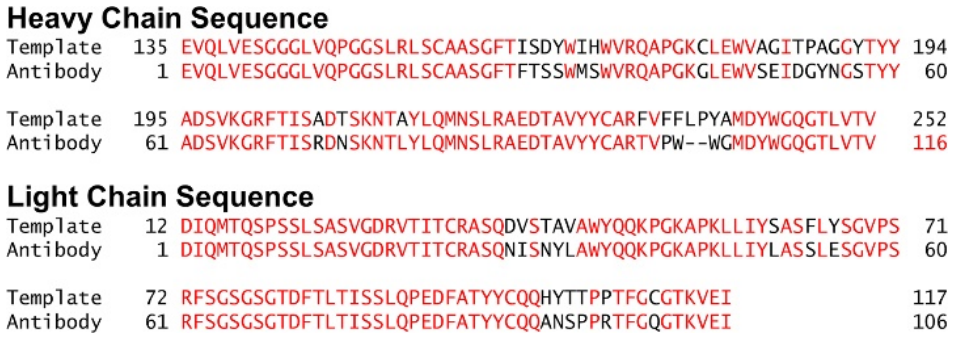


**Figure S2.** Amino acid sequence alignment between antibody against S275F RSV antigen and template in homology modeling. Identical amino acids are colored red.

**Table S5.** Primers for ssGFP production.

| Primer | Sequence (5' → 3') |
|---|---|
| 1 | GATATACATCATATGCATCATCACCACCACCAC |
| 2 | GGATCCTCCACCACTAGTCTTTTCGTTGGGATCTTTCG |
| 3 | ACTAGTGGTGGAGGATCCCGTGACCACATGGTC |
| 4 | CCAACCGCCGAATTCTCCTTTGTAGAGCTCATC |
| 5 | GACAAACAAACTAGTGGTGGAAATAGTGAACTGCT |
| 6 | TCCATTCTTGGATCCTGAAGTCGAACCACCACCGC |

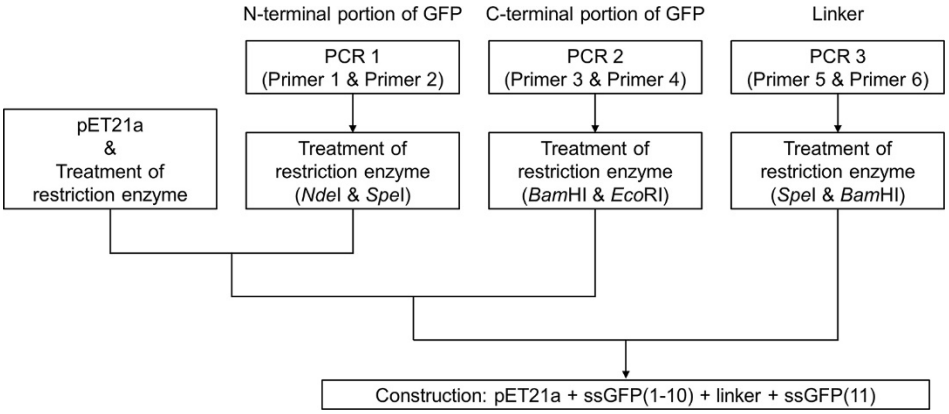


**Figure S3.** Scheme of vector construction for ssGFP.

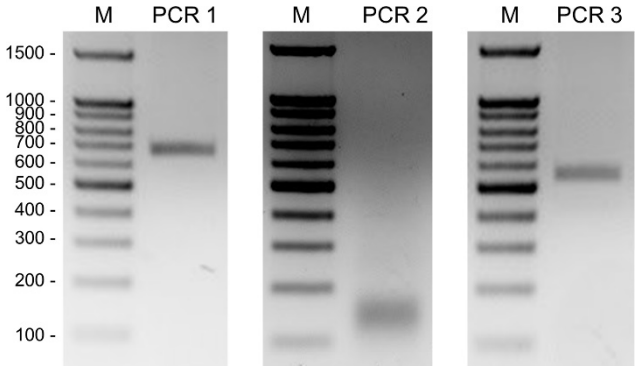


**Figure S4.** Gel electrophoresis results after PCR reactions.

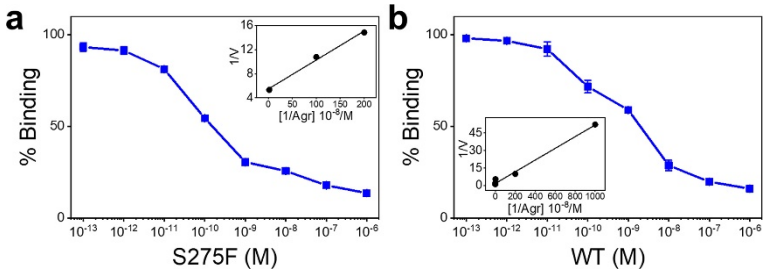


**Figure S5.** (a,b) Binding affinities of antibody (Ab94968) to (a) S275F and (b) WT RSV antigen by competitive ELISA. Insets represent Klotz plots. Data is represented as mean ± standard deviation of three measurements.

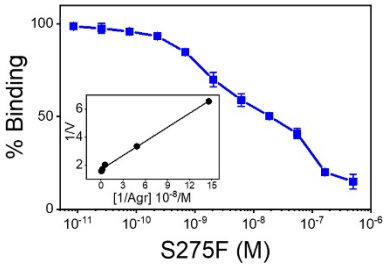


**Figure S6.** Binding affinity of antibody to S275F RSV antigen by competitive ELISA. Inset represents Klotz plots. Data is represented as mean ± standard deviation of three measurements.

**Binding Modes of S275F and WT RSV Epitopes in CDRs of Antibody**

The calculated binding modes of the S275F and WT epitopes in CDRs of the antibody are compared in Figure S7. In the antibody-S275F complex, Lys272 of the S275F mutant epitope formed two hydrogen bonds with the side chains of L-N31 and L-Y32 of the antibody. The side chain butylammonium ion (Lys272) of the mutant epitope acted as a hydrogen bond donor to the side chains of L-N31 and L-Y32. Moreover, the hydrophobic interactions between the Val278 of the S275F epitope and H-V100, H-P101, and H-W103 of the antibody were also detected in the antibody-S275F complex. In the antibody-WT complex, the side chain hydroxyl moiety of Ser30 in the light chain (L-S30) and the backbone aminocarbonyl oxygen of Pro101 in the heavy chain (H-P101) donated a hydrogen bond to the backbone aminocarbonyl oxygen of Ile280 and received the same from the side chain hydroxyl group of Ser275. In addition, the hydrophobic interactions between Val278 of the WT epitope and the aromatic residues of the antibody (L-Y32 and H-W103) were similar to those in the antibody-S275F complex. Notably, the binding mode of the S275F mutant epitope differed from that of the WT in that the phenyl ring of the mutated Phe275 was accommodated within a small hydrophobic pocket comprising the side chains of nonpolar residues in the light chain (L-Y49 and L-L50) and heavy chain (H-P101, H-W102, and H-W103). Because the number of hydrogen bonds in the two complexes was same, the strengthening of hydrophobic interactions in the CDRs of the antibody may explain the increase in the antibody-binding affinity resulting from the substitution of Phe for Ser at residue 275 of the RSV F protein.

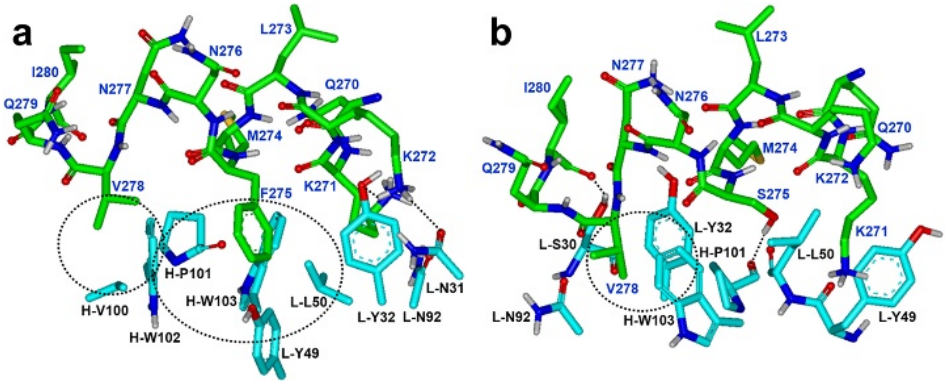


**Figure S7.** Calculated binding modes of (a) S275F and (b) WT RSV epitopes in CDRs of antibody. Dotted lines and circles indicate hydrogen bonds and hydrophobic interactions, respectively.

**Identification of S275F and WT RSV Antigens using ssGFP-Antibody-Cy5 System Chip**

The Cy5-conjugated antibody was prepared using NHS ester amine reaction, and the ssGFP was immobilized on an aldehyde glass slide. Next, the Cy5-conjugated antibody was coated on the ssGFP-immobilized glass and washed, which led to the formation of the ssGFP-antibody-Cy5 system chip. After preparing the ssGFP-antibody-Cy5 system chip, the S275F and WT RSV antigens were allowed to react on the chip and washed (Figure S8a). Moreover, when the S275F RSV antigen was reacted on the ssGFP-antibody-Cy5 chip, the mutant antigen bound to the Cy5-conjugated antibody and was released from the chip. The residual ssGFP emitted green fluorescence. In contrast, the ssGFP-antibody-Cy5 complex was retained on the glass after reacting with the WT RSV antigen, and Cy5 emitted red fluorescence signals. Figure S8b shows the fluorescence images of the ssGFP-antibody-Cy5 chip after detecting the S275F and WT RSV antigens. The green signals were clearly detected in the presence of the mutant RSV antigen, whereas red signals were detected in the presence of the WT antigen.

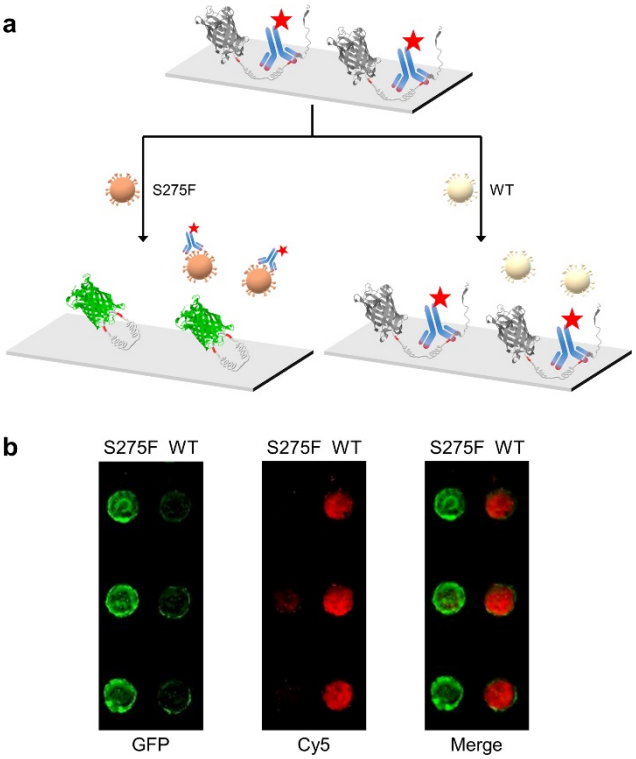


**Figure S8.** (a) Schematic illustration of S275F RSV antigen detection using ssGFP-antibody-Cy5 system chip. Green fluorescence signals are emitted in the presence of S275F RSV antigen and red signals in the presence of WT antigen. (b) Fluorescence images of ssGFP-antibody system chip after detection of RSV antigens (S275F and WT).

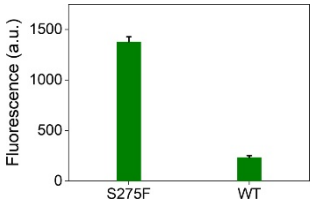


**Figure S9.** Fluorescence signals after detection of S275F and WT RSV antigens using ssGFP-antibody system. Data is represented as mean + standard deviation of three measurements.

**Dot-blot Test of S275F and WT VLPs using Palivizumab and Developed Antibody**

We tested whether the structure of the F protein in the VLP remained that in a real virus. As shown in Figure S10, palivizumab recognized only VLPs containing WT RSV F protein and not VLPs containing S275F as expected, whereas the developed antibody recognized only VLPs containing S275F and not VLPs containing WT. Therefore, we concluded that the VLPs were well-structured and properly assembled.

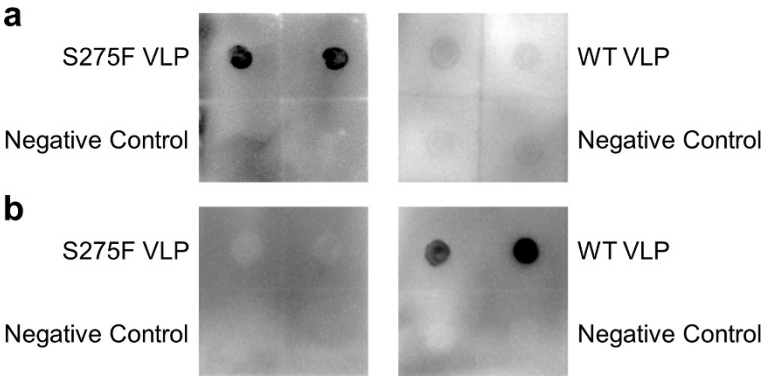


**Figure S10.** (a,b) Dot blot images after interaction of (a) developed antibody and (b) palivizumab with VLPs. Negative control is medium.